

**Structure of a model dye/titania interface:
Geometry of benzoate on rutile-TiO₂ (110)(1×1)**

W. Busayaporn^{1,2,3}, D.A. Duncan^{4†}, F. Allegretti⁴, A. Wander², M. Bech^{5‡}, P.J. Møller^{5§}, B.P.
Doyle^{6**}, N.M. Harrison^{2,7}, G. Thornton⁸, R. Lindsay^{1*}

¹*Corrosion and Protection Centre, School of Materials, The University of Manchester,
Sackville Street, Manchester, M13 9PL, UK*

²*STFC, Daresbury Laboratory, Daresbury, Warrington WA4 4AD, UK*

³*Synchrotron Light Research Institute, Nakhon Ratchasima 30000, Thailand*

⁴*Physik-Department E20, Technische Universität München,
James-Franck Str. 1, D-85748 Garching, Germany*

⁵*Department of Chemistry, University of Copenhagen, Universtetsparken 5,
DK 2100 Copenhagen Ø, Denmark*

⁶*IOM CNR Laboratorio TASC, Stada Statale 14, km. 163,5, 34149 Basovizza (TS), Italy*

⁷*Department of Chemistry, Imperial College London, Exhibition Road, London SW7 2AZ, UK*
⁸*London Centre for Nanotechnology and Chemistry Department,
University College London, 20 Gordon Street, London WC1H 0AJ, UK*

Corresponding Author:

Robert Lindsay

Tel: +44 161 306 4824

Fax: +44 161 306 4865

Email: robert.lindsay@manchester.ac.uk

[†] Diamond Light Source, Harwell Science and Innovation Campus, Didcot, Oxfordshire, OX11 0DE, UK

[‡] Department of Medical Radiation Physics, Clinical Sciences Lund, Lund University, SE-21185 Lund, Sweden

[§] Deceased.

^{**} Department of Physics, University of Johannesburg, PO Box 524, Auckland Park, 2006, South Africa

Abstract

Scanned-energy mode photoelectron diffraction (PhD) and *ab initio* density functional theory (DFT) calculations have been employed to investigate the adsorption geometry of benzoate ($[\text{C}_6\text{H}_5\text{COO}]^-$) on rutile- $\text{TiO}_2(110)(1\times 1)$. PhD data indicate that the benzoate moiety binds to the surface through both of its oxygen atoms to two adjacent five-fold surface titanium atoms in an essentially upright geometry. Moreover, its phenyl (C_6H_5^-) and carboxylate ($[-\text{COO}]^-$) groups are determined to be coplanar, being aligned along the $[001]$ azimuth. This experimental result is consistent with the benzoate geometry emerging from DFT calculations conducted for laterally rather well separated adsorbates. At shorter inter-adsorbate distances, the theoretical modeling predicts a more tilted and twisted adsorption geometry, where the phenyl and carboxylate groups are no longer coplanar, i.e. inter-adsorbate interactions influence the configuration of adsorbed benzoate.

Keywords: Chemisorption; Surface structure; Titanium oxide; Carboxylic acid; Single crystal surface; Photoelectron Diffraction

Introduction

Motivated to a large extent by the employment of the carboxyl (-COOH) containing molecules as solar harvesters in TiO₂-based dye-sensitized solar cells, there is significant ongoing activity seeking to elucidate the interaction of such species with single crystal TiO₂ surfaces (see, for example, Refs.¹⁻⁴). To date, most progress has been achieved for the simplest -COOH containing molecule, namely formic acid (HCOOH), on the prototypical rutile TiO₂(110)(1×1) surface^{2,5-21}. On this substrate, it is well known that at room temperature formic acid adsorbs dissociatively, i.e.



forming a (2×1) overlayer at a saturation coverage of approximately 0.5 monolayer (ML)^{5,6,12,15}; 1 ML corresponds to one formate per surface 5-fold Ti (Ti_{5c}). Furthermore, the geometry of this adsorbed formate species has been determined through both photoelectron diffraction (PhD) and quantitative low energy electron diffraction (LEED-IV) measurements^{18,20}, including high precision quantification of bond lengths and angles. Figure 1 illustrates the adsorption geometry resulting from these two studies, where formate binds to the surface in a bridging-bidentate mode through both of its oxygen atoms to two adjacent Ti_{5c}'s, so that its molecular plane lies parallel to the rows of bridging oxygen atoms (i.e. along the [001] direction). Currently, similar structural information is largely absent for other -COOH containing species (glycine is one exception²¹), with geometrical details typically being restricted to angular orientation from near edge X-ray absorption fine structure (NEXAFS) data and lateral location from scanning probe microscopy (SPM) images (see Ref.²², and Refs. therein]. In this study we address this issue, applying the well-established structural technique scanned-energy mode PhD^{23,24} to probe the adsorption geometry of benzoate ([C₆H₅COO]⁻) on TiO₂(110)(1×1). Complementary *ab initio* density functional theory (DFT) calculations are also presented to corroborate the experimental results, as well as to explore the influence of benzoate coverage on adsorption geometry.

Analogous to the dissociative adsorption of formic acid on $\text{TiO}_2(110)(1\times 1)$, benzoic acid ($\text{C}_6\text{H}_5\text{COOH}$), which consists of both a phenyl ring (C_6H_5-) and a carboxylic ($[-\text{COOH}]$) group, can lose its acidic hydrogen to form benzoate ($[\text{C}_6\text{H}_5\text{COO}]^-$) on this substrate^{2,4,25-30}. An initial study of this adsorbate system, employing a combination of scanning tunneling microscopy (STM), LEED, and electron stimulated desorption ion angular distribution (ESDIAD), reported a (2×1) overlayer, with benzoate oriented such that its principal axis lies more or less along the surface normal^{25,26}. Furthermore, it was deduced that benzoate dimers, and even trimers, are formed, through edge-to-face phenyl ring (C-H/ π -system) interactions, i.e. the phenyl ring of the adsorbed benzoate can adopt more than one azimuthal orientation. This latter conclusion is supported by other NEXAFS and STM measurements²⁷. Similarly, more recent work suggests that exposure of $\text{TiO}_2(110)(1\times 1)$ to benzoic acid, both in ultra high vacuum (UHV)^{4,29} and in aqueous solution², does not always simply result in a planar (and upright) benzoate species. These studies are, however, not in complete agreement, e.g. vibrational data in Ref.⁴ are interpreted as indicating that benzoate-dimerization occurs as 0.5 ML coverage is approached, whereas STM images²⁹ suggest that dimers are not a feature of this coverage regime. On this basis, further effort is required to gain a more robust insight into the configuration of the adsorbed benzoate. Scanned-energy mode PhD, in tandem with first principles modeling, is an appropriate approach for achieving this end.

Methods

Experimental work was undertaken on the BEAR beam line³¹ of the ELETTRA synchrotron radiation facility in Trieste, Italy. The beam line's UHV end station (base pressure $\sim 1 \times 10^{-10}$ mbar), equipped with facilities for sample transfer, cleaning, dosing, and characterization, was employed³². Photoelectron spectra were acquired with a 66 mm mean radius spherical deflector electron energy analyzer³², which was positioned such that the angle between its entrance lens and the incoming photon beam was 60° in the horizontal plane. The angular resolution of the analyzer was set to 1° for this work.

In situ preparation of $\text{TiO}_2(110)(1\times 1)$ involved repeated cycles of Ar^+ bombardment and annealing at ~ 1000 K. Surface cleanliness and order were monitored by photoelectron spectroscopy (PES) and low energy electron diffraction (LEED), respectively. Exposure to benzoic acid (99.9%, Riedel-de Haën) was undertaken with the TiO_2 substrate at room temperature by allowing its vapor to enter the UHV chamber through a high precision leak valve; an *in situ* mass spectrometer was used to check the purity of this benzoic acid vapor. Prior to admittance, the benzoic acid was thoroughly degassed via repeated sublimation-deposition cycles. During dosing the glass vial containing the benzoic acid and the rest of the gas line were gently heated with a hot air gun to achieve a sufficient partial pressure of benzoic acid vapor.

All of the PhD data presented in this paper were acquired from $\text{TiO}_2(110)(1\times 1)$ surfaces exposed initially to between $\sim 2 \times 10^{-5}$ mbar s and $\sim 5 \times 10^{-5}$ mbar s of benzoic acid. Such dosing resulted in a saturation-coverage of adsorbed benzoate, as determined from PES spectra. The benzoate overlayer was not, however, entirely stable in the synchrotron radiation (SR) beam, rather it desorbed progressively with time. Nevertheless, data acquisition was feasible as the overlayer degradation was slow enough to facilitate measurement through a combination of periodically moving the sample to expose fresh areas of the surface to the SR beam, and re-dosing with benzoic acid.

Scanned-energy mode PhD spectra from both O 1s and C 1s core levels were acquired. These data were obtained by measuring a series of energy distribution curves (EDCs), at intervals of 4 eV in photon energy, over a kinetic energy range of $\sim 50 - 300$ eV. Similar PhD spectra were collected in a number of different emission directions, ranging from 0° (normal emission) to 60° in polar angle in both the $[001]$, and $[1\bar{1}0]$ azimuths. To reduce these raw PhD data to a form suitable for structure determination a standard methodology was applied^{23,24}. Briefly, the intensity of each of the peaks present in an EDC is extracted by fitting with appropriate functions i.e. a Gaussian line shape function for each core level feature, a Gaussian broadened step function, and an experimental background template to

account for the inelastic background and any Auger features. These intensities ($I(E)$) are then plotted as a function of photoelectron kinetic energy and normalized to give a modulation function ($\chi(E)$), which can be used for structure determination. $\chi(E)$ is defined as follows:

$$\chi(E) = \frac{I(E) - I_0(E)}{I_0(E)}. \quad [1]$$

$I_0(E)$ is a smooth spline function, representing non-diffractive intensity and instrumental factors.

All DFT calculations have been performed using the CRYSTAL program³³, in which the crystalline orbitals are expanded as a linear combination of atom-centered Gaussian orbitals, the basis set. The titanium and oxygen ions are described using triple valence all-electron basis sets contracted as 86-411G** and 8-411G**, respectively. These basis sets were developed in previous studies of the bulk and surfaces of titania in which a systematic hierarchy of all-electron basis sets was used to quantify the effects of using a finite basis set^{34,35}. The C and H atoms of the benzoate are described using basis sets of a similar quality, namely 6311G* and 821G*, respectively. Electronic exchange and correlation were approximated in the local density approximation (LDA). This choice is to avoid the instability of the rutile TiO₂ phase inherent in calculations using generalized gradient approximation (GGA) or hybrid-exchange (e.g. PBE0 or B3LYP) functionals³⁶. This approach results in bulk unit cell parameters of $a = 4.567 \text{ \AA}$ and $c = 2.935 \text{ \AA}$, which are very similar (within 1 %) to those determined experimentally³⁷. Calculations have been performed on slabs periodic in two dimensions (parallel to the TiO₂(110) surface), but finite in the third. On the basis of test calculations, a centrosymmetric substrate slab comprising 15 layers was adopted, with benzoate (plus acidic hydrogen) adsorbed on both slab faces. To assess the impact of adsorbate coverage/arrangement, a range of supercells (unit cells) were used, namely (2×1), (2×2) and (4×1). During energy minimization, all atoms were allowed to move, except for those Ti and O atoms at the slab centre.

Results

O 1s and C 1s core level PES data, acquired from $\text{TiO}_2(110)(1\times 1)$ following a saturation exposure of benzoic acid, are displayed in Figure 2. Both spectra are consistent with those reported previously²⁸, indicating the integrity of the overlayer preparation. The O 1s spectrum is comprised of a primary peak and a lower kinetic energy shoulder, which are assigned to substrate oxygen atoms (O_{ox}), and a combination of carboxylate oxygen (O_{carb}) and OH_b (see Figure 1), respectively^{18,28}. Two peaks, separated by approximately 3.9 eV, are visible in the C 1s spectrum. The more intense, higher kinetic energy feature is associated with the carbon atoms of the phenyl ring (C_{ph}), and the other arises from the carboxylate carbon (C_{carb}).

Concerning PhD data from the O 1s core level, modulation functions for each component (O_{ox} and $\text{O}_{\text{carb}}/\text{OH}_b$) have been compared with data acquired previously from $\text{TiO}_2(110)(1\times 1)$ -formate¹⁸ to qualitatively determine the adsorption site of benzoate. This comparison is shown in Figure 3. Focusing initially on the O_{ox} data, it is evident that the modulations are very similar, i.e. they are essentially independent of adsorbate (benzoate or formate). Given that the O_{ox} 1s peak is due to substrate oxygen, this result is to be expected, and so confirms the reliability of the current PhD measurements. More notably, the PhD spectra of the $\text{O}_{\text{carb}}/\text{OH}_b$ component for the two adsorbate systems are also rather similar, strongly suggesting that both benzoate and formate exhibit similar binding sites on $\text{TiO}_2(110)(1\times 1)$, i.e. attachment to the surface is through both of the carboxylate oxygen atoms to two adjacent five-fold surface titanium atoms; scanned-energy mode PhD data are normally most sensitive to nearest neighbor atoms below the emitting atom^{23,24}. Such a conclusion is in agreement with previous proposals/predictions of the local adsorption geometry of benzoate on $\text{TiO}_2(110)(1\times 1)$ ^{2,4,25-30}.

Turning to PhD data from the C 1s core level, a more quantitative structure determination, using the modulation functions extracted from the C_{ph} component, has been performed; C_{carb}

1s modulation functions were not suitable for analysis due to the low intensity of the PES peak. This effort involved the usual trial-and-error methodology of generating simulated modulation functions for a systematic series of adsorption geometries, searching for the best fit between experiment and theory as measured using a reliability factor (R-factor)^{23,24}; this R-factor is defined such that a value of 0 corresponds to perfect agreement between theory and experiment, a value of 1 corresponds to no correlation and a value of 2 to anti-correlation. Computer code capable of electron multiple scattering calculations, developed by Fritzsche³⁸⁻⁴⁰, was employed to generate the theoretical modulations functions.

As a starting point for generating simulated C_{ph} 1s modulation functions, the high symmetry [C₆H₅COO]⁻ adsorption geometry depicted in Figure 4 was initially adopted, which is consistent with the binding site concluded above from qualitative analysis of O 1s PhD data. To identify the optimum structure, a global search algorithm, specifically a particle swarm optimization (PSO)⁴¹, was used. A number of parameters were optimized during this process, including those defining the location of the benzoate, as well as others describing vibrations. These parameters are detailed in the following list:

- (i) Twist of phenyl ring away from [001] azimuth (φ);
- (ii) Out-of-plane (of molecule) tilt of the center of mass of the phenyl ring (θ);
- (iii) In-plane (of molecule) tilt of the center of mass of the phenyl ring (ϕ);
- (iv) C-C bond length within the phenyl group (C_{ph}-C_{ph});
- (v) Bond length between carboxylate carbon and phenyl group carbon to which it is directly attached (C_{ph}-C_{carb});
- (vi) Vertical height of the carboxylate carbon (C_{carb}) atom above the carboxylate oxygen (O_{carb}) atoms;
- (vii) Lateral separation of the carboxylate oxygen (O_{carb}) atoms;
- (viii) Vertical height of carboxylate oxygen (O_{carb}) atoms above the five fold Ti (Ti_{5c}) atoms;
- (ix) Root mean square (RMS) amplitude of isotropic vibrations of the carboxylate

oxygen (O_{carb}) and carbon (C_{carb}) atoms;

- (x) RMS amplitude and in plane:out-of-plane anisotropy ratio of vibrations of phenyl carbon (C_{ph}) atoms.

It should be noted that during structure optimization the local symmetries of the phenyl group and C_{carb} atom were maintained (i.e. planar, with all bond lengths/angles in the phenyl group being equal), as was the adsorbed symmetry of the two carboxylate oxygen atoms (i.e. they remain located directly above the Ti_{5c} row). No such constraints were implemented for the *ab initio* modeling.

As regards describing the angular geometry of the phenyl ring relative to the substrate, which is defined by parameters (i) – (iii) above (φ , θ , and ϕ), we have adopted the so-called intrinsic Tait-Bryan formalism (closely related to Euler angles). According to this description, φ , θ , and ϕ relate two independent coordinate systems xyz and XYZ , which are fixed relative to the substrate and adsorbate (phenyl ring and C_{carb}), respectively. More explicitly, as shown in Figure 4, φ , θ , and ϕ each correspond to a rotation of the phenyl ring (and C_{carb}) about a particular molecular axis, namely Z , X , and Y , respectively; the origin of the XYZ coordinate system is the center of mass of the two carboxylate oxygen atoms. In order to achieve the final orientation the sequence in which the rotations are applied is uniquely defined, i.e. $\varphi \rightarrow \theta \rightarrow \phi$, as illustrated in Figure 5 (N.B. $(\varphi, \theta, \phi) = (0^\circ, 0^\circ, 0^\circ)$ for the geometry depicted in Figure 4).

Concerning structure optimization, the majority of the parameters listed above had little impact upon the quality of the experiment-theory fit, i.e. varying such a parameter did not cause the R-factor to exceed the variance²⁴. Only φ , θ , and ϕ , along with the $C_{\text{ph}}-C_{\text{ph}}$ and $C_{\text{carb}}-C_{\text{ph}}$ bond lengths, exhibited any significance. Figure 6 displays a comparison of the experimental C_{ph} 1s modulation functions with the best-fit theoretical simulations resulting from optimization of these parameters within the parameter-space outlined above; a total of 7200 structures were trialed during optimization. There is reasonable agreement between the

experimental and theoretical modulations functions, with the R-factor being 0.42. Table I lists corresponding optimum values of parameters. Inspection of this table indicates that the plane of phenyl ring is coplanar with that of the carboxylate group ($\varphi = 5^\circ \pm 20^\circ$), and that the entire benzoate moiety is oriented upright within experimental error ($\theta = 10^\circ \pm 15^\circ$ and $\phi = 5^\circ \pm 4^\circ$). Hence the optimum structure mirrors that depicted in Figure 4. Concerning the $C_{\text{ph}}-C_{\text{ph}}$ and $C_{\text{carb}}-C_{\text{ph}}$ bond lengths, which were found to be $1.42 \pm 0.04 \text{ \AA}$ and $1.50 \pm 0.15 \text{ \AA}$, respectively, they agree well with equivalent bond lengths determined for both a molecular crystal of benzoic acid⁴², and benzoic acid in the gas phase⁴³.

Turning to *ab initio* modeling, initially we focus on calculations undertaken to simulate lower adsorbate coverage, where the benzoate moieties are laterally rather well separated. For this purpose, as shown in Figure 7 (A), a (4×1) supercell was used with the benzoate coverage being 0.25 ML ($(4 \times 1)/0.25 \text{ ML}$). Calculations were undertaken for two different locations (relative to the adsorbed benzoate) of the acidic hydrogen on the bridging oxygen rows, which are labeled (1) and (2) in Figure 7 (A). The optimum geometry obtained is shown in Figure 7 (B). Visually, the adsorption geometry adopted by the benzoate is analogous to that found from PhD. Indeed, as illustrated in Table I, the values of φ , θ and ϕ agree very well with those obtained experimentally. Concerning the acidic hydrogen, it was found that location (1) was energetically somewhat more favorable, i.e. there is a preference for the bridging hydroxyl to be adjacent to the adsorbed benzoate.

Further calculations have been performed for adsorbed benzoate with smaller lateral inter-adsorbate separation. More specifically, $(2 \times 2)/0.25 \text{ ML}$ and $(2 \times 1)/0.5 \text{ ML}$ supercells have been considered, as depicted in Figures 8 (A) and (B), respectively. We note that for both of these systems, in contrast to the $(4 \times 1)/0.25 \text{ ML}$ overlayer, the benzoate species are close packed along the [001] azimuth. Figure 8 (C) and (D) depict the optimum geometries emerging from the calculations. In both cases, the phenyl ring displays significantly more twisting/tilting away than the near upright adsorption geometry predicted for the $(4 \times 1)/0.25 \text{ ML}$ overlayer (Figure 7 (b)). On this basis, it can be concluded that the shorter inter-adsorbate

distance in the [001] azimuth results in modification of the angular geometry of the adsorbed benzoate, i.e the phenyl rings twist/tilt in the $(2 \times 2)/0.25 \text{ ML}$ and $(2 \times 1)/0.5 \text{ ML}$ overlayers to optimize lateral interactions. Table I lists the values of φ , θ and ϕ for both overlayers, which are almost identical.

One remaining adsorption scenario is that where the phenyl group of the adsorbed benzoate can adopt more than one angular orientation. Such a possibility has been tested theoretically using the two supercells illustrated in Figures 9 (A) and (B), namely $(4 \times 1)/0.5 \text{ ML}$ and $(2 \times 2)/0.5 \text{ ML}$, which both display phenyl groups oriented along the [001] and $[1\bar{1}0]$ azimuths. For each of these initial structures, energy minimization resulted in adoption of a (2×1) -like structure, in which every adsorbate is more or less identical, i.e. there is a single adsorbate geometry, which is analogous to the twisted/tilted structures shown in Figure 8. The PhD data support this result, in that attempts to input a phenyl ring oriented parallel to the $[1\bar{1}0]$ azimuth into the PhD modulation simulations leads to an appreciable increase in R-factor. This sensitivity to phenyl ring geometry can be appreciated by comparing the simulated modulation functions shown in Figure 10. Displayed data were generated (60° polar emission angle) for a phenyl ring oriented in either the [001] or $[1\bar{1}0]$ azimuth, and it is evident that the amplitude of the modulations varies significantly as a function of this angular geometry. Referring to the experimental data in Figure 6, the modulations at 60° are only appreciable in the [001] azimuth, i.e. there is no evidence for more than one azimuthal orientation of the phenyl ring.

Turning to a comparison of the nearly upright/coplanar structure emerging from PhD with the results of *ab initio* modeling, there is clearly excellent agreement between experiment and the adsorbate structure predicted for the $(4 \times 1)/0.25 \text{ ML}$ overlayer (see Table I). In contrast, the PhD structure is apparently somewhat less consistent with the more twisted/tilted benzoate geometry found for the $(2 \times 1)/0.5 \text{ ML}$ overlayer, which was *a priori* presumed to be the surface phase probed experimentally; it should be pointed out the error bars ascribed to the experimentally determined values of φ , θ and ϕ (see Table I) indicate that the two structures

are not strictly distinct. Results from a relatively recent STM study²⁹, however, suggest that *room temperature* adsorption of benzoic acid on $\text{TiO}_2(110)(1\times 1)$ may lead to a saturation coverage significantly less than expected, i.e. ~ 0.2 ML rather than 0.5 ML; adsorption undertaken at a somewhat elevated substrate temperature (370 K) was found to result in a higher benzoate coverage, much closer to 0.5 ML. Hence, the PhD data, acquired following *room temperature* adsorption, may very well have been acquired from ~ 0.2 ML of benzoate, rather than ~ 0.5 ML, which would explain the nearly upright/coplanar optimum adsorbate geometry. It should be noted that it was not possible to estimate the benzoate coverage from PES core level data with sufficient precision to differentiate between 0.2 ML and 0.5 ML, i.e. the associated error bar is too large.

Regarding the origin of the lower saturation coverage (~ 0.2 ML), one possible explanation emerges from benzoic acid forming hydrogen bonded dimers in the vapor phase⁴⁴, as illustrated in Figure 11. Given this scenario, it may be that sufficient adsorbate free area is required on the $\text{TiO}_2(110)(1\times 1)$ surface to facilitate initial adsorption/decoupling of the dimer prior to dissociative adsorption of the monomer. Consequently, adsorption is terminated far below saturation of all Ti_{5c} sites. At somewhat elevated substrate temperatures, increased surface diffusion may allow greater coverages to be achieved.

Finally, we wish to compare the results of our current study with previous efforts to elucidate the adsorption geometry of benzoate on $\text{TiO}_2(110)(1\times 1)$ ^{2,4,25-27,29,30}. Initially, we want to re-emphasise that our PhD data are inconsistent with any overlayer structures involving benzoates where their phenyl groups exhibit two or more azimuthal orientations, a scenario suggested initially in Refs.²⁵⁻²⁷. Moreover, our theoretical modeling demonstrates that such configurations are energetically unfavourable. In contrast, our experimentally determined upright/planar benzoate geometry is consistent with that deduced on the basis of vibrational data acquired from a low coverage (< 0.5 ML) phase of benzoate⁴. Furthermore, in that study lower symmetry (twisted/tilted) benzoate species potentially exist at room temperature saturation coverage (0.5 ML), which seemingly matches our *ab initio* prediction. One

outstanding issue arising from this comparison concerns the surface coverages achieved in the two studies. More specifically, given the above discussion about saturation coverage at room temperature (i.e. ~ 0.2 ML rather than ~ 0.5 ML), the 0.5 ML coverage reported in Ref.⁴ requires some commentary. Simply, it may be that this coverage estimation is inaccurate, although we would not then expect lower symmetry benzoate species to be present. Alternatively, some variation in experimental methodology has facilitated an increased adsorbate coverage, e.g. the substrate was above room temperature during benzoic acid exposure.

Concerning STM studies^{2,25-27,29} in which images have been interpreted to indicate the presence of twisted/tilted benzoate species (e.g. through dimer/trimer formation), substrate temperature/coverage may again underpin these observations. It may also be, however, that extracting the geometry of benzoate, or any adsorbate for that matter, from such images is not so straightforward, as explicitly indicated in another study involving STM imaging of benzoate on $\text{TiO}_2(110)(1\times 1)^{30}$, and that such deductions should be critically evaluated.

Conclusion

In summary, a combination of scanned-energy mode PhD and *ab initio* modeling has been applied to elucidate the adsorption geometry of benzoate ($[\text{C}_6\text{H}_5\text{COO}]^-$) on rutile- $\text{TiO}_2(110)(1\times 1)$. A comparison of current O 1s core level PhD data with those acquired from $\text{TiO}_2(110)(1\times 1)$ -formate¹⁸ indicates analogous interfacial bonding, i.e. the benzoate moiety binds to the surface through both of its oxygen atoms to two adjacent five-fold surface titanium atoms. Theoretical simulation of C 1s PhD modulations demonstrate that this benzoate moiety is essentially upright on the surface, and adopts a planar configuration with its phenyl (C_6H_5-) and carboxylate ($[-\text{COO}]^-$) groups aligned along the [001] azimuth. A similar benzoate geometry emerges from DFT calculations conducted for laterally rather well separated adsorbates. For shorter inter-adsorbate distances, a more tilted/twisted adsorption geometry, where the phenyl and carboxylate groups are no longer coplanar, is predicted.

However, contradicting a previous assertion²⁵⁻²⁷, overlayer structures comprised of benzoate species with their phenyl groups displaying more than one angular orientation are found to be energetically unfavorable.

Supporting Information

CIF files containing the atomic coordinates for the $(4\times 1)/0.25$ ML, $(2\times 2)/0.25$ ML and $(2\times 1)/0.5$ ML optimized slabs. This material is available free of charge via the Internet at <http://pubs.acs.org>

Acknowledgements

The authors wish to thank ELETTRA staff for their support. The PhD measurements were facilitated by the European Community's Seventh Framework Programme (FP7/2007-2013) under grant agreement n° 226716. In addition, through membership of the UK's HEC Materials Chemistry Consortium, which is funded by EPSRC (EP/L000202), this work used the ARCHER UK National Supercomputing Service (<http://www.archer.ac.uk>). DAD would like to acknowledge funding from the Alexander von Humboldt foundation.

References

1. Heckel, W.; Elsner, B. A. M.; Schulz, C.; Müller, S. The Role of Hydrogen on the Adsorption Behaviour of Carboxylic Acid on TiO₂ Surfaces. *J. Phys. Chem. C* **2014**, *118*, 10771-10779.
2. Grinter, D. C.; Woolcot, T.; Pang, C. L.; Thornton, G. Ordered Carboxylates on TiO₂(110) Formed at Aqueous Interfaces. *J. Phys. Chem Lett.* **2014**, *5*, 4265-4269.
3. Yu, Y.Y.; Gong, X.-Q. Unique Adsorption Behaviours of Carboxylic Acids at Rutile-TiO₂(110). *Surf. Sci.* **2015**, *641*, 82-90.
4. Buchholz, M.; Xu, M.; Noei, H.; Weidler, P.; Nefedov, A.; Fink, K; Wang, Y.; Wöll, C. Interaction of Carboxylic Acids with Rutile TiO₂(110): IR-Investigations of Terephthalic and Benzoic Acid Adsorbed on a Single Crystal Substrate. *Surf. Sci.* **2016**, *643*, 117-123.
5. Onishi, H.; Aruga, T.; Iwasawa, Y. Switchover of Reaction Paths in the Catalytic Decomposition of Formic Acid on TiO₂(110) Surface. *J. Catal.* **1994**, *146*, 557-567.
6. Henderson, M. A. Complexity in the Decomposition of Formic Acid on the TiO₂(110) Surface. *J. Phys. Chem. B* **1997**, *101*, 221-229.
7. Wang, L.-Q.; Ferris, K. F.; Shultz, A. N.; Baer, D. R.; Engelhard, M. H. Interactions of HCOOH with Stoichiometric and Defective TiO₂(110) Surfaces. *Surf. Sci.* **1997**, *380*, 352-364.
8. Ahdjoudj, J.; Minot, C. A Theoretical Study of HCO₂H Adsorption on TiO₂(110). *Catal. Lett.* **1997**, *46*, 83-91.
9. Chambers, S. A.; Thevuthasan, S.; Kim, Y. J.; Herman, G. S.; Wang, Z.; Tober, E.; Ynzunza, R.; Morais, J.; Peden, C. H. F.; Ferris, K.; Fadley, C. S. Chemisorption Geometry of Formate on TiO₂(110) by Photoelectron Diffraction. *Chem. Phys. Lett.* **1997**, *267*, 51-57.
10. Bates, S. P.; Kresse, G.; Gillan, M. J. The Adsorption and Dissociation of ROH Molecules on TiO₂(110). *Surf. Sci.* **1998**, *409*, 336-349.

11. Thevuthasan, S.; Herman, G. S.; Kim, Y.J.; Chambers, S. A.; Peden, C. H. F.; Wang, Z.; Ynzunza, R. X.; Tober, E. D.; Morais, J.; Fadley, C. S. The Structure of Formate on TiO₂(110) by Scanned-Energy and Scanned-Angle Photoelectron Diffraction. *Surf. Sci.* **1998**, *401*, 261-268.
12. Hayden, B. E.; King, A.; Newton M. A. Fourier Transform Reflection-Absorption IR Spectroscopy Study of Formate Adsorption on TiO₂(110). *J. Phys. Chem. B* **1999**, *103*, 203-208.
13. Käckell, P.; Terakura, K. First-Principle Analysis of the Dissociative Adsorption of Formic Acid on Rutile TiO₂(110). *Appl. Surf. Sci.* **2000**, *166*, 370-375.
14. Käckell, P.; Terakura, K. Dissociative Adsorption of Formic Acid and Diffusion of Formate on the TiO₂(110) Surface; the Role of Hydrogen. *Surf. Sci.* **2000**, *461*, 191-198.
15. Chang, Z.; Thornton, G. Reactivity of Thin-Film TiO₂(110). *Surf. Sci.* **2000**, *462*, 68-76.
16. Gutiérrez-Sosa, A.; Martínez-Escolano P.; Raza, H.; Lindsay, R.; Wincott, P. L.; Thornton, G. Orientation of Carboxylates on TiO₂(110). *Surf. Sci.* **2001**, *471*, 163-169.
17. Bowker, M.; Stone, P.; Bennett, R.; Perkins, N. Formic Acid Adsorption and Decomposition on TiO₂(110) and on Pd/TiO₂(110) Model Catalysts. *Surf. Sci.* **2001**, *511*, 435-448.
18. Sayago, D. I.; Polcik, M.; Lindsay, R.; Toomes, R. L.; Hoeft, J. T.; Kittel, M.; Woodruff, D. P. Structure Determination of Formic Acid Reaction Products on TiO₂(110). *J. Phys. Chem. B* **2004**, *108*, 14316-14323.
19. Aizawa, M.; Morikawa, Y.; Namai, Y.; Morikawa, H.; Iwasawa, Y. Oxygen Vacancy Promoting Catalytic Dehydration of Formic Acid on TiO₂(110) by in Situ Scanning Tunneling Microscopic Observation. *J. Phys. Chem. B* **2005**, *109*, 18831-18838.
20. Lindsay, R.; Tomić, S.; Wander, A.; García-Méndez, M.; Thornton, G. Low Energy Electron Diffraction Study of TiO₂(110)(2×1)-[HCOO]⁻. *J. Phys. Chem. C*, **2008**, *112*, 14154-14157.

21. Lerotholi, T. J.; Kröger, E. A.; Knight, M. J.; Unterberger, W.; Hogan, K.; Jackson, D. C.; Lamont, C. L. A.; Woodruff, D. P. Adsorption Structure of Glycine on TiO₂(110): A Photoelectron Diffraction Determination. *Surf. Sci.* **2009**, *603*, 2305-2311.
22. Pang, C. L.; Lindsay, R.; Thornton, G. Structure of Clean and Adsorbate-Covered Single Crystal Rutile TiO₂ Surfaces. *Chem. Rev.* **2013**, *113*, 3887-3948.
23. Woodruff, D. P.; Bradshaw, A. M. Adsorbate Structure Determination on Surfaces using Photoelectron Diffraction. *Rep. Prog. Phys.* **1994**, *57*, 1029-1080.
24. Woodruff, D. P. Adsorbate Structure Determination using Photoelectron Diffraction: Methods and Applications. *Surf. Sci. Rep.* **2007**, *62*, 1-38.
25. Guo, Q.; Cocks, I.; Williams E. M. The Adsorption of Benzoic Acid on a TiO₂(110) Surface Studied using STM, ESDIAD and LEED. *Surf. Sci.* **1997**, *393*, 1-11.
26. Guo, Q.; Williams E. M. The Effect of Adsorbate-Adsorbate Interaction on the Structure of Chemisorbed Overlayers on TiO₂(110). *Surf. Sci.* **1999**, *433-435*, 322-326.
27. Schnadt, J.; Schiessling, J.; O'Shea, J. N.; Gray, S. M.; Patthey, L.; Johansson, M. K.-J.; Shi, M.; Krampaský, J.; Åhlund, J.; Karlsson, P. G.; Persson, P.; Mårtensson, N.; Brühwiler, P. A. Structural Study of Adsorption of Isonicotinic Acid and Related Molecules on Rutile TiO₂(110) I: XAS and STM. *Surf. Sci.* **2003**, *540*, 39-54.
28. Schnadt, J.; O'Shea, J. N.; Patthey, L.; Schiessling, J.; Krampaský, J.; Shi, M.; G.; Mårtensson, N.; Brühwiler, P. A. Structural Study of Adsorption of Isonicotinic Acid and Related Molecules on Rutile TiO₂(110) II: XPS. *Surf. Sci.* **2003**, *544*, 74-86.
29. Grinter, D. C.; Nickels, P.; Woolcot, T.; Basahel, S. N.; Obaid, A. Y.; Al-Ghamdi, A. A.; El-Mossalamy, E.-S. H.; Alyoubi, A. O.; Thornton, G. Binding of a Benzoate Dye-Molecule Analogue to Rutile Titanium Dioxide Surfaces. *J. Phys. Chem. C* **2012**, *116*, 1020-1026.
30. Landis, E. C.; Jensen, S. C.; Phillips, K. R.; Friend, C. M. Photostability and Thermal Decomposition of Benzoic Acid on TiO₂. *J. Phys. Chem. C* **2012**, *116*, 21508-21513.
31. Nannarone, S.; Borgatti, F.; De Luisa, A.; Doyle, B. P.; Gazzadi, G. C.; Giglia, A.; Finetti, P.; Mahne, N.; Pasquali, L.; Pedio, M.; Selvaggi, G.; Naletto, G.; Pelizzo, M.

- G.; Tondello, G. The BEAR Beamline at Elettra. *AIP Conference Proceedings*; AIP Publishing, 2004; Vol. 705, pp 450-453.
32. Pasquali, L.; De Luisa A.; Nannorone, S. The UHV Experimental Chamber for Optical Measurements (Reflectivity and Absorption) and Angle Resolved Photoemission of the BEAR Beamline at ELETTRA. *AIP Conference Proceedings*; AIP Publishing, 2004; Vol. 705, pp 1142-1145.
33. Dovesi, R.; Saunders, V. R.; Roetti, C.; Orlando, R.; Zicovich-Wilson, C.M.; Pascale, F.; Civalleri, B.; Doll, K.; Harrison, N. M.; Bush, I.J.; D'Arco, P.; Llunell, M.; Causà, M.; Noël, Y. CRYSTAL14 User's Manual (University of Torino, Torino, 2014).
34. Sanches, F. F.; Mallia, G.; Liborio, L.; Diebold, U.; Harrison, N. M. Hybrid Exchange Density Functional Study of Vicinal Anatase TiO₂ Surfaces. *Phys. Rev. B*, **2014**, *89*, 245309.
35. Muscat, J.; Swamy, V.; Harrison, N. M. First-Principles Calculations of the Phase Stability of TiO₂, *Phys. Rev. B*, **2002**, *65*, 224112.
36. Montanari, B.; Harrison, N.M. Pressure-Induced Instabilities in Bulk TiO₂ Rutile. *J. Phys.: Condensed Matter*, **2004**, *16*, 273.
37. Burdett, J. K.; Hughbanks, T.; Miller, G. J.; Richardson, Jr., J.W.; Smith J. V. Structural-Electronic Relationships in Inorganic Solids: Powder Neutron Diffraction Studies of the Rutile and Anatase Polymorphs of Titanium Dioxide at 15 and 295 K. *J. Am. Chem. Soc.* **1987**, *109*, 3639-3646.
38. Fritzsche, V. Approximations for Photoelectron Scattering. *Surf. Sci.* **1989**, *213*, 648-656.
39. Fritzsche, V. Calculations of Auger Electron Diffraction at a Ni(111) Surface. *J. Phys.: Condens Matter* **1990**, *2*, 8734-9747.
40. Fritzsche, V. Consequences of a Finite Energy Resolution for Photoelectron Diffraction Spectra. *Surf. Sci.* **1992**, *265*, 187-195.

41. Duncan, D. A.; Choi, J. I. J.; Woodruff, D. P. Global Search Algorithms in Surface Structure Determination using Photoelectron Diffraction. *Surf. Sci.* **2012**, *606*, 278-284.
42. Feld, R.; Lehmann, M. S.; Muir, K. W.; Speakman, J. C. The Crystal Structure of Benzoic Acid: a Redetermination with X-rays at Room Temperature; a Summary of Neutron-Diffraction Work at Temperatures down to 5 K. *Z. Kristallogr.* **1981**, *157*, 215-231.
43. Aarset, K.; Page, E. M.; Rice, D. A. Molecular Structures of Benzoic Acid and 2-Hydroxybenzoic Acid, Obtained by Gas-Phase Electron Diffraction and Theoretical Calculations. *J. Phys. Chem. A* **2006**, *110*, 9014-9019.
44. Bakker, J. M.; Mac Aleese, L.; von Helden, G.; Meijer, G. The Infrared Absorption Spectrum of the Gas Phase Neutral Benzoic Acid Monomer and Dimer. *J. Chem. Phys.* **2003**, *119*, 11180-11185.

Table I. Optimum values of structural parameters for TiO₂(110)-benzoate emerging from best fit of experimental C_{ph} 1s PhD data, along with those emerging from DFT calculations for (4×1)/0.25 ML, (2×2)/0.25 ML and (2×1)/0.5 ML supercells. φ , θ and ϕ are illustrated in Figures 4 and 5.

Parameter	Optimum Value			
	PhD	DFT	DFT	DFT
		(4×1)/0.25 ML	(2×2)/0.25 ML	(2×1)/0.5 ML
φ	$5 \pm 20^\circ$	0°	20°	20°
θ	$10 \pm 15^\circ$	5°	23°	24°
ϕ	$5 \pm 4^\circ$	0°	1°	1°
C _{ph} - C _{ph}	$1.42 \pm 0.04 \text{ \AA}$	$1.38 - 1.40 \text{ \AA}$	$1.38 - 1.40 \text{ \AA}$	1.39 \AA
C _{carb} - C _{ph}	$1.50 \pm 0.15 \text{ \AA}$	1.46 \AA	1.46 \AA	1.47 \AA

Figure Captions

- Figure 1** Ball and stick model illustrating the adsorption geometry of $[\text{HCOO}]^-$ on $\text{TiO}_2(110)(1\times 1)$, as determined from PhD and LEED-IV data^{18,20}. Also indicated is the location of the acidic hydrogen (H^+), resulting from HCOOH dissociative adsorption, which was identified in the PhD study¹⁸, i.e. it is bonded to a bridging oxygen (O_b), forming a surface bridging hydroxyl (OH_b). A 5-fold Ti atom (Ti_{5c}) is also labelled.
- Figure 2** O 1s (left panel) and C 1s (right panel) core level PES spectra acquired following a saturation exposure of benzoic acid. Data were acquired at normal emission. See text for an explanation of the peak labels.
- Figure 3** O 1s scanned-energy mode PhD modulation functions; emission directions are indicated. Modulations from $\text{TiO}_2(110)(1\times 1)$ – benzoate (thin lines) and $\text{TiO}_2(110)(1\times 1)$ -formate¹⁸ (bold lines) are compared. Labelling denotes the O 1s PES core level component (O_{ox} or $\text{O}_{\text{carb}/\text{OH}_b}$) from which the data have been extracted. The somewhat poorer signal to noise exhibited by the benzoate system data is simply a result of differences in the measurement facilities employed, including the lower photon flux delivered by the BEAR beam line.
- Figure 4** Ball and stick model illustrating the initial adsorption geometry of $[\text{C}_6\text{H}_5\text{COO}]^-$ on $\text{TiO}_2(110)(1\times 1)$ adopted for generating simulated C_{ph} 1s PhD modulation functions. The two coordinate systems xyz and XYZ, which are fixed relative to the substrate and adsorbate (phenyl ring/ C_{carb}), respectively, are indicated. Also shown are the rotations induced by non-zero values of θ , ϕ and φ about X, Y, and Z, respectively. The origin of XYZ coordinate system is the center of mass of the two carboxylate oxygen atoms.

Figure 5 Illustration of rotations (φ , θ , and ϕ), and order in which they are applied, to describe angular geometry of phenyl ring (and C_{carb}). XYZ coordinate system is fixed relative to the adsorbate (phenyl ring and C_{carb}), i.e. it moves (including rotation) with the adsorbate. The origin of XYZ coordinate system is the center of mass of the two carboxylate oxygen atoms.

Figure 6 Comparison of the experimental C_{ph} 1s PhD modulation functions (bold line) with the best-fit theoretical simulations (thin line). Note the significant difference in the experimental modulations acquired at 60° polar emission angle in the two azimuths, which is only reproduced in the theoretical simulations for small values of φ (twist of phenyl ring about principal axis of benzoate relative to [001] azimuth).

Figure 7 (A) Plan view of $(4 \times 1)/0.25$ ML benzoate supercell employed for *ab initio* modeling of adsorption geometry. Calculations were undertaken for two different locations (relative to the adsorbed benzoate) of the acidic hydrogen on the bridging oxygen rows, which are labelled (1) and (2). (B) Illustration of theoretically predicted $(4 \times 1)/0.25$ ML structure.

Figure 8 (A) Plan view of $(2 \times 2)/0.25$ ML benzoate supercell employed for *ab initio* modeling of adsorption geometry. (B) Plan view of $(2 \times 1)/0.5$ ML benzoate supercell employed for *ab initio* modeling of adsorption geometry. (C) Illustration of theoretically predicted $(2 \times 2)/0.25$ ML structure. (D) Illustration of theoretically predicted $(2 \times 1)/0.5$ ML structure.

Figure 9 (A) Plan view of $(4 \times 1)/0.5$ ML benzoate supercell employed for *ab initio* modeling of adsorption geometry. (B) Plan view of $(2 \times 2)/0.5$ ML benzoate supercell employed for *ab initio* modeling of adsorption geometry.

Figure 10 Theoretical C_{ph} 1s PhD modulation functions (60° polar emission angle in both measurement azimuths) generated for an adsorbed benzoate with its phenyl ring oriented in either the $[001]$ (left hand side) or $[\bar{1}\bar{1}0]$ (right hand side) azimuth, as depicted in corresponding illustrations. Experimental data are displayed in Figure 6.

Figure 11 Ball and stick model of a hydrogen bonded benzoic acid dimer.

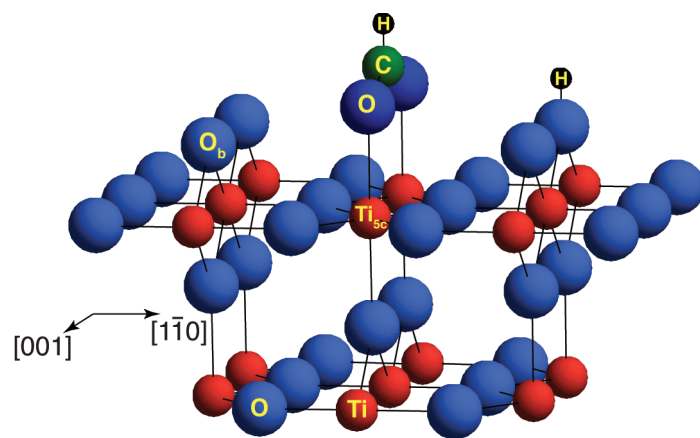


Figure 1

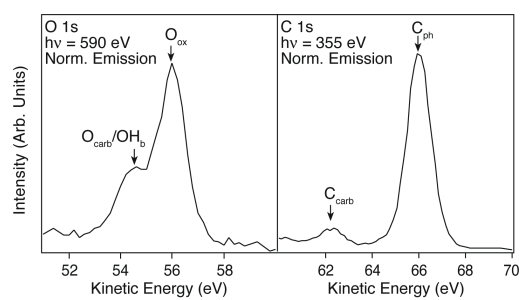


Figure 2

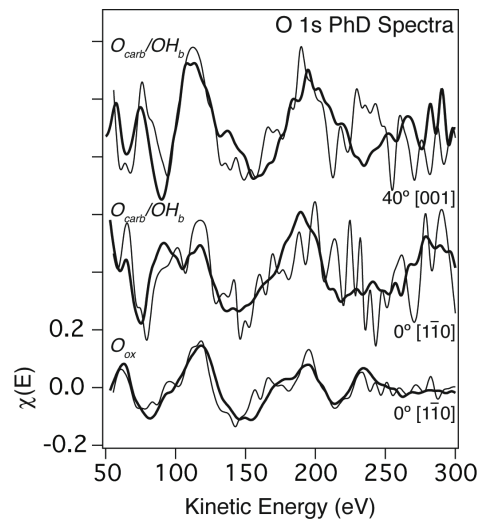


Figure 3

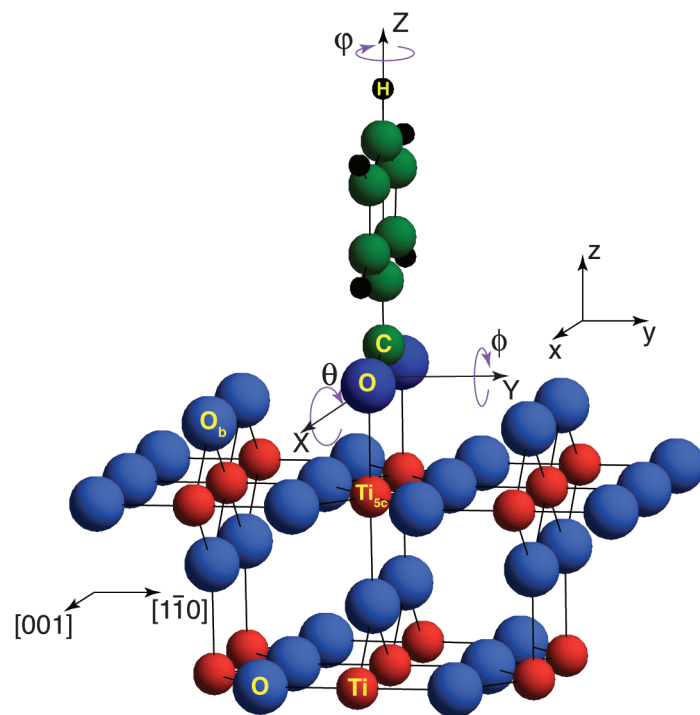


Figure 4

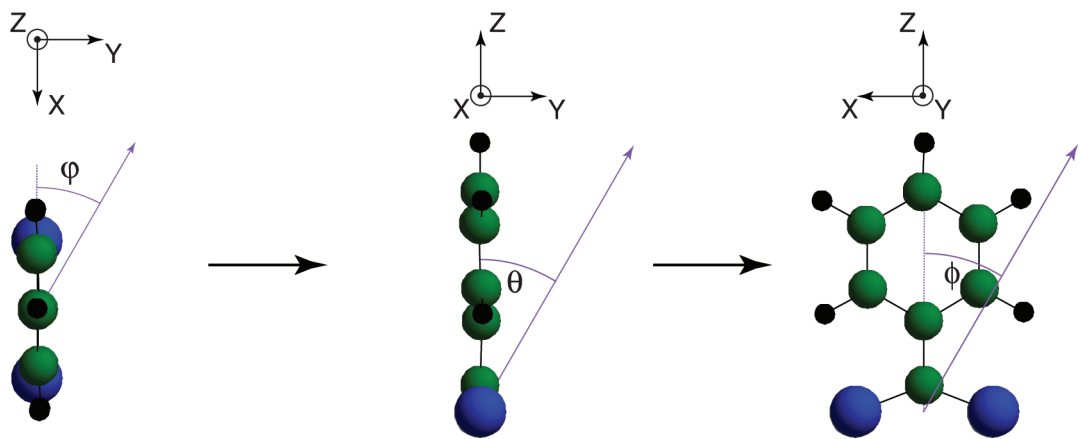


Figure 5

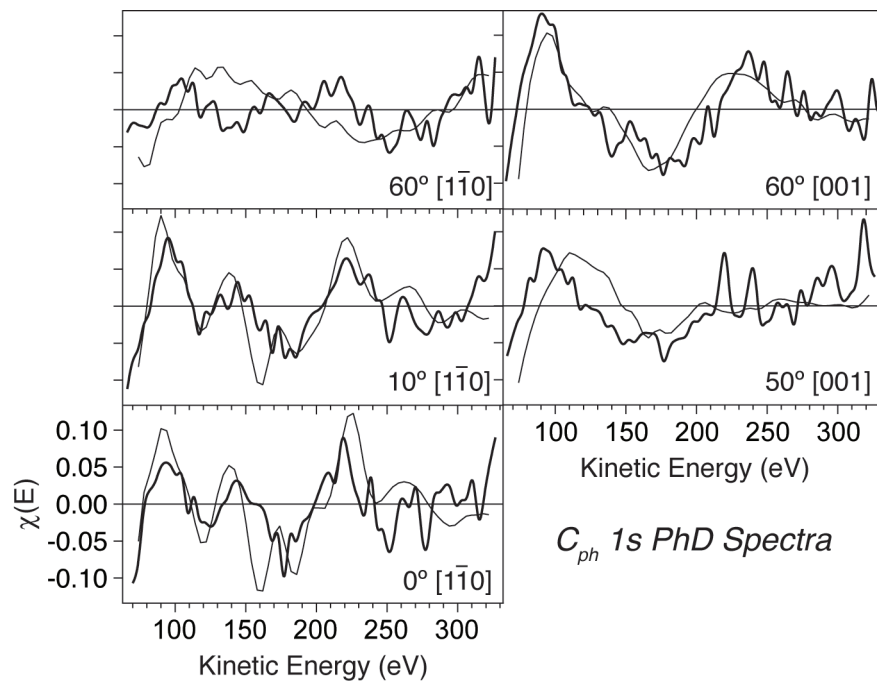


Figure 6

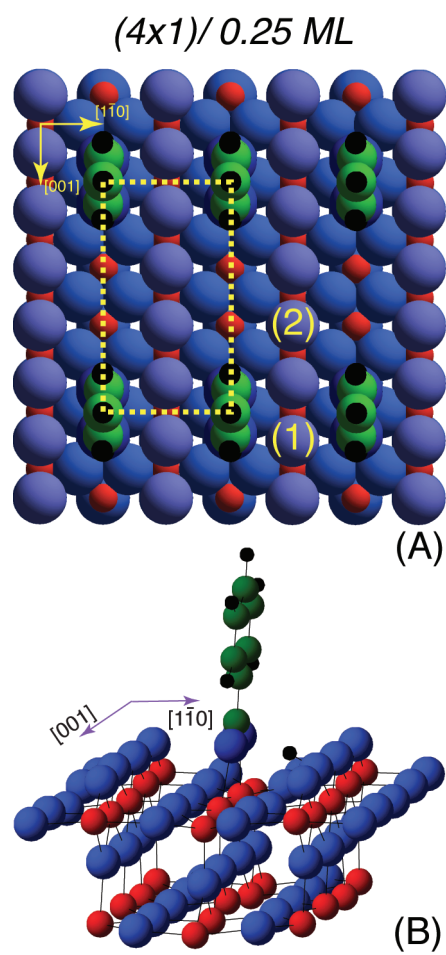


Figure 7

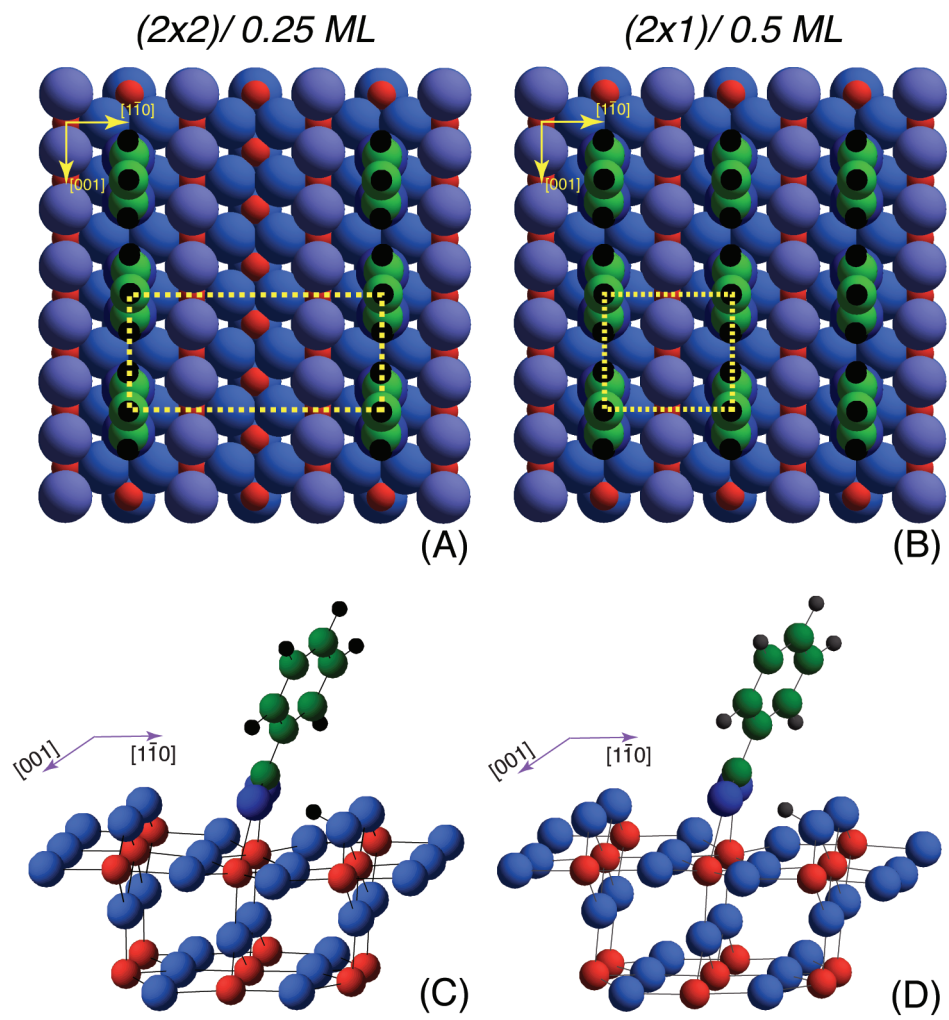


Figure 8

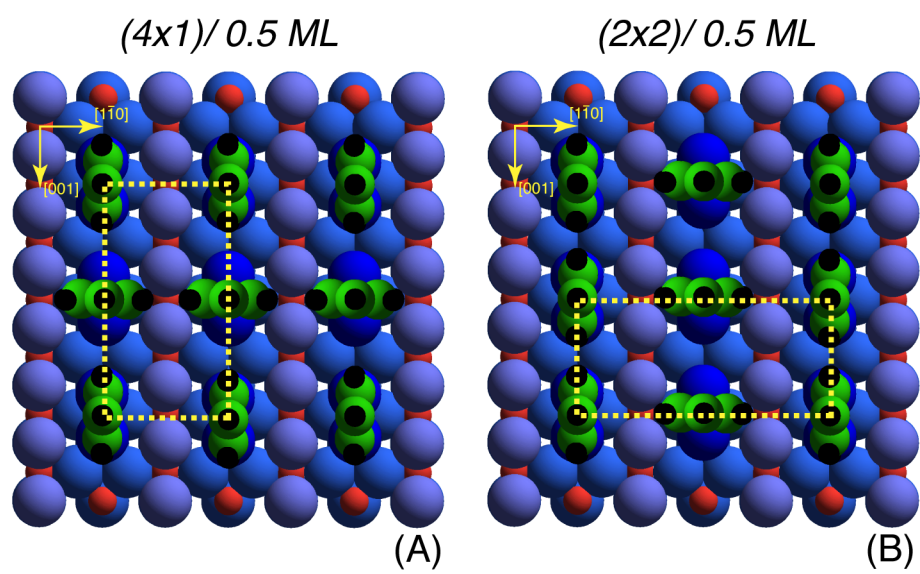


Figure 9

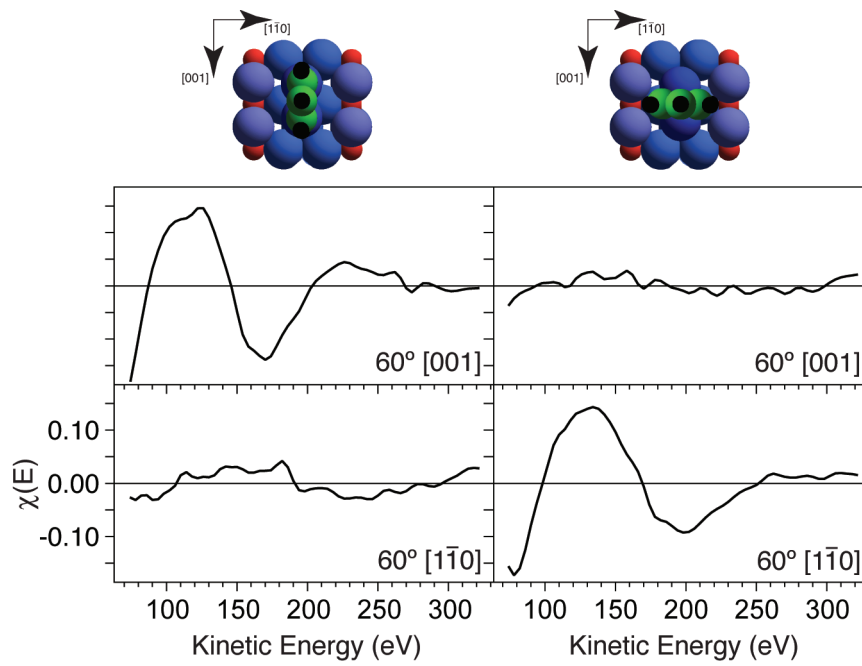


Figure 10

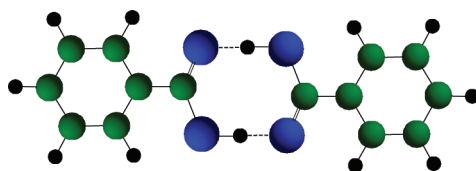


Figure 11

TOC Figure:

